

Laser MicroJet® Technology - Fundamental Study and Highlights of its Latest Applications

T. A. Mai, N. U. Kling, N. Vago, B. Richerzhagen, K. Stay*

Synova SA, Ch. de la Dent-d'Oche 1, CH-1024 Ecublens, Switzerland

Phone +41 21 694 35 00; fax +41 21 694 35 01

E-mail: stay@synova.ch

**Synova USA Inc., 48521 Warm Springs Blvd, suite 314, Fremont CA 94359, USA*

Phone +1 510 438 8900; fax +1 510 438 8805

Abstract

The water jet-guided laser technology (known as Laser MicroJet® or LMJ) has been rapidly adapted with success in various industries, validating its unique advantages against conventional laser material processing. Matured applications are, for example, dicing, drilling and slotting of semiconductor wafers, cutting of coronary stents, drilling of stencil and OLED masks, cutting of difficult-to-machine (e.g. copper, aluminium, polyamide) or hard materials, such as PCD/WC for tool inserts. This cold, clean and damage free machining technology allows a high speed, precise fabrication of intricate structures, providing exceptional aspect ratios and finishing quality.

A well-rounded understanding of the jet stability characteristics is very important to enhance the performance of the LMJ technology. This paper will present investigative results of the fundamental behaviour of a hair-thin water jet, namely jet velocity, jet breakup, and jet stability at different parameters. The propagation and intensity distribution of a laser beam coupled in a low pressure, laminar water jet with various coupling conditions are theoretically and experimentally investigated as well. In the final part of this paper, some recent machining examples of the LMJ technology will be highlighted.

Keywords: Water guided laser, micromachining, cutting, drilling, structuring, jet stability

Introduction

In a very short period of time the new principle of a water jet-guided laser for micromachining has securely established itself, and is making a big impact in industry [1]. The principle of using a water jet as a waveguide, for guiding a light beam was first observed and reported by D. Colladon in 1842 in Geneva [2]. The phenomena has now been practically applied to focussing a laser beam into and guiding it through a hair fine jet of low-pressure water, by means of the total internal reflection of the laser beam by the wall of the water jet. This results in having a laser cutting mechanism, which has an extremely long cutting distance and not restricted to the short working range of a conventional focussed dry laser.

The diameter of the jet is relatively large (25 – 150 µm) when compared to the wavelength of the lasers (≈ 1 µm), so the water jet can be considered to be a multimode fibre. Propagation of light in multimode fibres is usually characterized by a finite number of guided modes, refractive and tunnelling leaky modes that are partially guided, and a continuum of radiation modes [3]. Many theoretical aspects of propagation of waves in cylindrical waveguides are discussed in literature [4].

The stability of the water jet, characterized by the breakup length, is limited by increasing water surface waves. They are due to initial perturbations [5] and also due to the laser induced breakup [6]. In this paper, the propagation and intensity distribution of a low power and coherent laser light in the water jet waveguide is investigated.

The jet is produced by forcing the water, under low pressure, through a sharp edged nozzle made from either diamond or sapphire mounted in the coupling unit (see Figure 1).

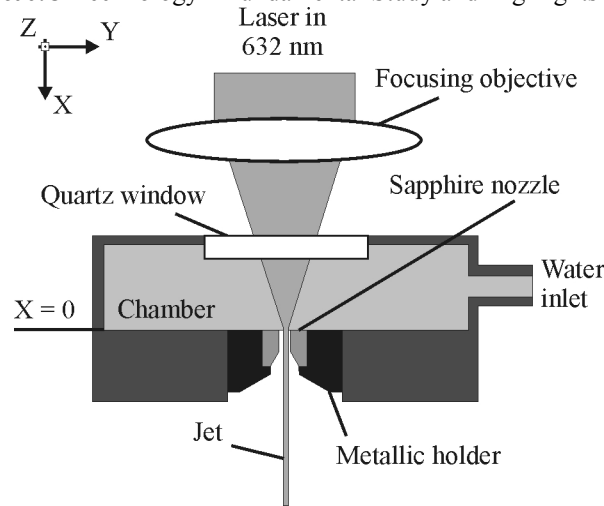


Fig. 1 Schematic of the coupling unit

Due to the vena contracta effect, the diameter of the resulting water jet is about 20% smaller than the nozzle diameter [7]. The coupling unit consists of a quartz window, a chamber and a nozzle holder where nozzles of different orifice diameters (presently 25-150 μm) can be installed.

The liquid jet breakup phenomena can be divided into regimes that reflect differences in the jet appearance as the operating conditions are changed. These regimes can be associated with different combination of forces acting on the jet and leading to its breakup such as liquid inertia, surface tension and aerodynamic forces. A common method to categorize the breakup regimes is to consider the breakup length (L_b) as a function of the mean jet velocity, U_j . The function $L_b(U_j)$ gives the so called breakup curve.

A typical configuration of the breakup curve obtained in experiments is presented in Figure 2 [8].

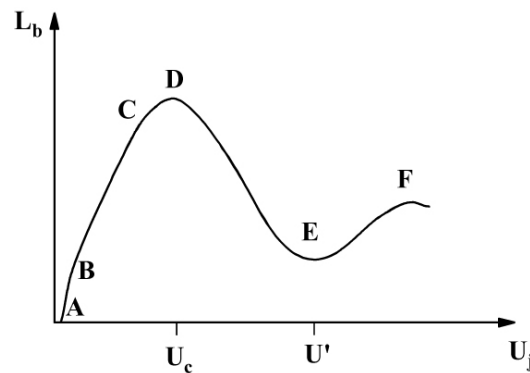


Fig. 2 Empirical breakup curve (L =Breakup length, U =Speed)

The actual breakup mode is strongly related to the velocity difference $\Delta U = |U_j - U_a|$ between the liquid jet and the surrounding atmosphere. This difference controls the level of aerodynamic forces. For the case of a low velocity jet in an ambient gas at rest, the aerodynamic forces are negligible: the process is governed by surface tension, which promotes the growth of axisymmetric long wavelength disturbances on the jet surface. This capillary pinching breaks up the jet into drops with a diameter comparable to the jet diameter. This is called the Rayleigh mode regime: here the breakup length increases linearly with U_j until it reaches a maximum, the critical point (point D in Figure 2).

The decrease of the breakup length beyond point D is actually related to the increasing influence of aerodynamic forces. The mechanism of breakup changes progressively from axisymmetrical capillary pinching (varicose breakup) to asymmetrical sinuous breakup and then to wind loading. For high values of ΔU (high liquid or gas velocity), the instabilities lead the jet to break up into drops with diameters much smaller than the jet diameter. This latter corresponds to the Taylor mode or atomisation regime [9].

The destabilisation process changes in space and in time. This results in the fluctuation of the breakup length under constant working conditions (free jets).

The experimental investigations aiming to understand the mechanism of jet disintegration can be categorized as measurements of the local type and the global type. Local type measurements are concerned with the temporal evolution of the interfacial displacement of the jet at a particular downstream position using a laser beam interacting with a small portion of the liquid jet [10, 11]. For the global type measurements the entire jet, or a significant part of it, is spatially analysed [12, 13]. In this case a collimated beam of light illuminates the jet from behind creating a shadow image (shadowgraphy). The exposure time of the image must be short enough compared to the jet velocity to freeze the motion i.e. the movement during this time must be smaller than the resolution of the image. Manual or automatic image analysis can be used to determine the variation of the jet diameter or the breakup length.

For the investigation of high-speed microjets with velocity higher than 100 m/s and jet diameter smaller than 500 microns finding new methods is essential. In this case the classical measurement procedure (the shadowgraphy) gets difficult and expensive as ultra high-speed cameras or light sources are needed, and also time consuming because of the treatment of numerous pictures.

Coupling visible light into the water jet actually serves as a measurement tool for the breakup length of a wide variety of free jets. The jet guides the light until the point where the amplitude of surface waves is big enough to scatter out the light from the jet. Observing the jet from a direction perpendicular to its axis the appearing light indicates the location of breakup. This method of the global type visualizes the breakup point indirectly exploiting the wave guiding properties of liquid jets. Real time examination is possible as well as creating statistics of the breakup fluctuations.

The principle is the following. As a first step the light of a He-Ne laser is coupled into the water jet by means of a focusing lens. The jet behaves as a step index cylindrical waveguide as long as the surface waves are small enough to fulfil the requirement of total internal reflection (TIR) at the water-air interface. Because of the refraction index difference ($n_{\text{water}}=1.33$, $n_{\text{air}}=1$) the jet has a large numerical aperture: 0.879.

The second step is the determination of the breakup point by detection of the scattered light. Let us consider the propagation of the light in the jet during a short period of time while the jet moves infinitesimally. Where the surface wave amplitude exceeds a threshold level (depending on the numerical aperture of the coupling), the angle of incidence at the water-air interface reaches the critical angle of TIR. Then the light begins to scatter out of the jet nearly parallel to the surface as shown in Figure 3. Meanwhile the angle between the jet axis and the guided rays increases due to the successive reflections on the wavy surface. This effect and the further growth of the waves lead to the scattering-out of light at increasing angles with respect to the jet axis. Right before the disruption point the scattered rays leave the jet at 90 degrees. Observing the jet from a perpendicular direction to its axis the appearing light indicates the position of the breakup.

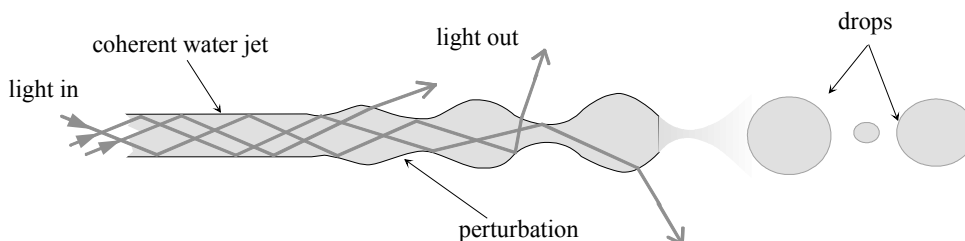


Fig. 3 The figure shows the process as the light scatters out of the water jet

Experimental Set-up

The following experiment demonstrates the efficiency of the method. The expanded light from a He-Ne laser ($\lambda = 632$ nm, 5 mW), was focused by a 46 mm focal length lens into the coupling unit through the window as shown in zone 1 of Figure 4. The coupling was achieved by means of moving stages for the focusing lens (x direction), and the coupling unit (y and z direction). Checking of the alignment is made using a monitoring CCD camera. Even in case of small jet diameter the red light scattered out of the jet makes the breakup event visible to the naked eye.

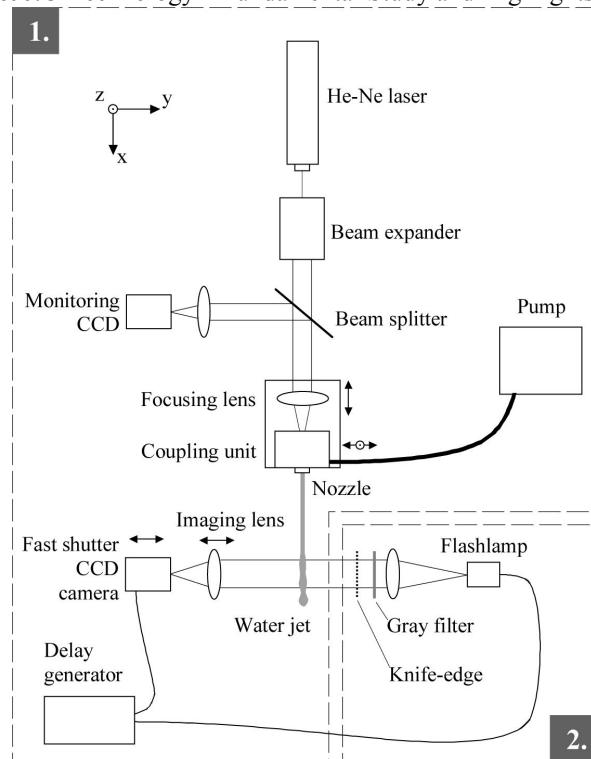


Fig. 4 Schematic of the integrated set-up. Zone 1: set-up for light coupling and imaging; Zone 2: backlighting arrangement for shadowgraphy

The breakup length detection with the coupled light and the shadowgraphy was performed by the same imaging system consisting of a black and white CCD-video camera with fast electronic shutter (1 μs minimum exposure time) and an 8 mm focal length objective. Both could be moved along the optical axis perpendicular to the jet, so that the magnification could be adjusted arbitrarily.

For the shadow imaging a 1 μs pulse duration flashlight provided parallel illumination by means of a condenser lens (see zone 2 in Figure 4). A delay generator drove the video camera and the flashlight. By adjusting the delay between the camera shutter and the flashlight, a 0.1 μs exposure time was achievable. The intensity and distribution of the backlighting was controlled with a grey filter and an adjustable knife-edge. High magnification images were taken of the jet at the breakup region with and without backlighting (Figures 5a) and 5b)).

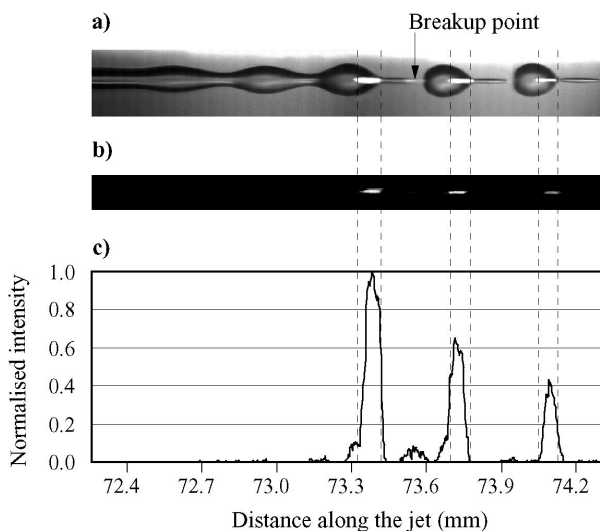


Fig. 5 a) Shadow image of a 40 micron radius jet with mean velocity of 60 m/s, with the scattered-out laser light; b) Image of the scattered light without backlighting; c) The intensity distribution of the scattered laser light from picture b)

One can see the axis-symmetric waves on the surface, which grow until the breakup. The breakup point is located 73.55 mm from the nozzle exit. There are two separated droplets shown in the image, the non-linear effect of ligament formation between the drops is also visible.

The laser light leaving the jet in the direction corresponding to the numerical aperture of the imaging objective forms bright stripes in the image. The breakup point is located between the two brightest stripes. Images made with the same setting without backlighting prove that the stripes are generated by the escaping laser light (see Figure 5b)).

At lower magnification, where the entire jet is visible, different exposure time images give the statistics of the breakup length for the corresponding time intervals. With short exposure time the instantaneous position of the breakup is obtainable. With long exposure (Figure 6) the intensity values superpose and the intensity profile provides the time the breakup point spent on a certain location. The result is the same as adding multiple short exposure images. Thus a single long exposure image yields a probability density function similar to the one Leroux et al. [14] created by treatment of thousands of images.

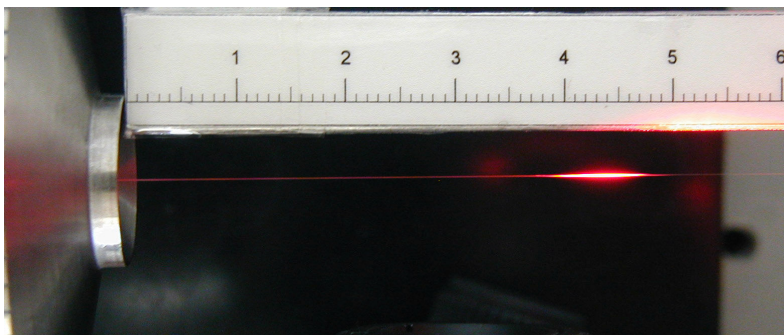


Fig. 6 Long time exposure of scattered laser light, with no back lighting, showing the intensity profile distribution of the breakup

With the light-guided method one can trace the position of the breakup point with a time resolution depending on the speed of the imaging, and create fast statistical analysis of the breakup fluctuation as well. The advantage of the technique is its speed and versatility. For instantaneous measurement it doesn't reach the precision of high-speed shadowgraphy, but it can be exploited for parameter ranges, where the shadowgraphy becomes difficult to use: small diameters, high jet velocities and strong breakup fluctuation.

To demonstrate the capabilities of this method the breakup curve of a 19 μm radius jet was measured until 325 m/s jet velocity. With long time exposure the probability distribution of the breakup length fluctuation was determined for different jet velocities. The maximum of the distribution was taken as the breakup length and plotted as the function of jet velocity (see Figure 7a)). The width of the fluctuation was also indicated.

The measured values follow the shape of the empirical breakup curve (see Figure 1). The breakup length grows linearly with the mean jet velocity until 200 m/s. Then the increase slows down and the curve reaches a maximum around 310 m/s: this is the critical velocity. The breakup length fluctuation shows increasing tendency towards higher jet velocities. In Figure 7b) standard high magnification shadow images show the jet shape close to the breakup for different velocities. The sharpness of the images is lower compared to Figure 5a) because of the high speed. The effect of the surrounding air can be examined for increasing jet velocities. At 175 m/s the breakup is axisymmetric, at 250 m/s small at 325 m/s stronger asymmetry is visible. The perturbation wavelength decreases with higher jet velocities.

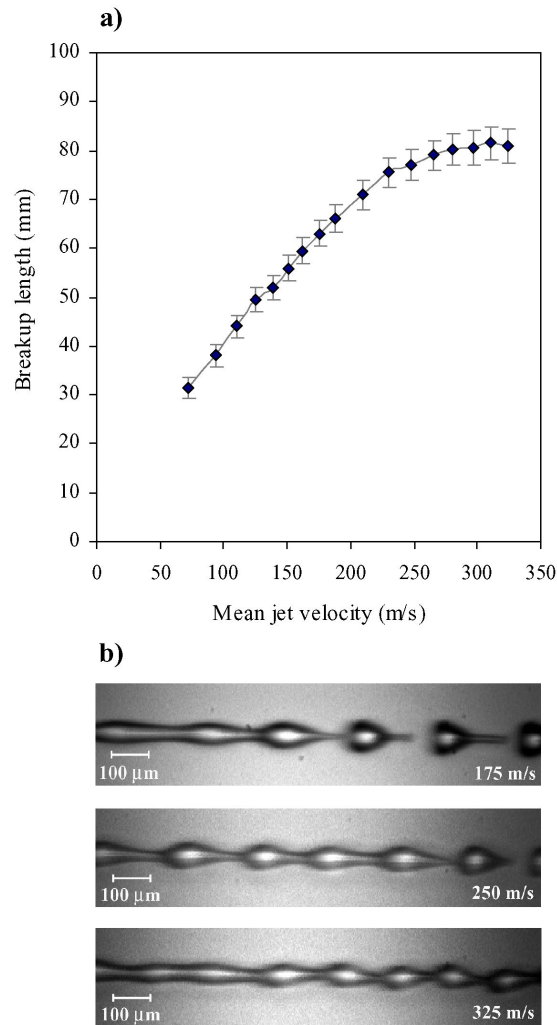


Fig. 7 a) Breakup curve of a 19 micron radius water jet measured with the light-guided technique; b) High magnification image of the jet at 175, 250 and 325 m/s jet velocities, without guided laser light

Concluding Remarks

In this paper we introduced an original technique for measuring the breakup length of free liquid jets with the help of coupled and guided light. The high magnification high-speed shadow images show that the light leaving the jet perpendicular to its axis indicates the breakup point. With long exposure imaging time statistics of the breakup fluctuation is automatically obtainable, independently of the jet size and speed, without high magnification or fast image acquisition. The feasibility was shown for a high-speed water jet, where the shadow imaging reaches its limits. The results presented show the capability of the method: immediate analysis is possible on the extent and properties of the breakup fluctuations for high-speed microjets.

Recent Micromachining Examples with the LMJ

The following non-exhaustive examples are given to demonstrate both the versatility and the high quality results obtained from the LMJ in everyday micromachining applications. The ability to cut thick materials cleanly, with narrow, perfectly parallel kerf walls, little or no heat affected zone (HAZ) and no contamination or deposition of ablated materials makes it the laser cutting tool of choice for the micromachining industry.

Solar Cell Edge Isolation

Edge isolation of solar cells, which can be performed by cutting a groove at the wafer edge as shown in Figure 8, is required to prevent shunts forming, which if present will seriously reduce the cells conversion efficiency. In this example, it was carried out with a UV 355nm laser, the nozzle and water jet diameters were 40 and 36 μm respectively. The groove depth varied from 20-25 μm , depending on the water pressure, and the kerf width was 40 μm . Cutting was carried out in a single pass at a speed of 300 to 350mm/s. Average laser power was 10.4W, which is approximately half the power required when the same speed is used with a 532nm laser, to achieve the same groove depth.

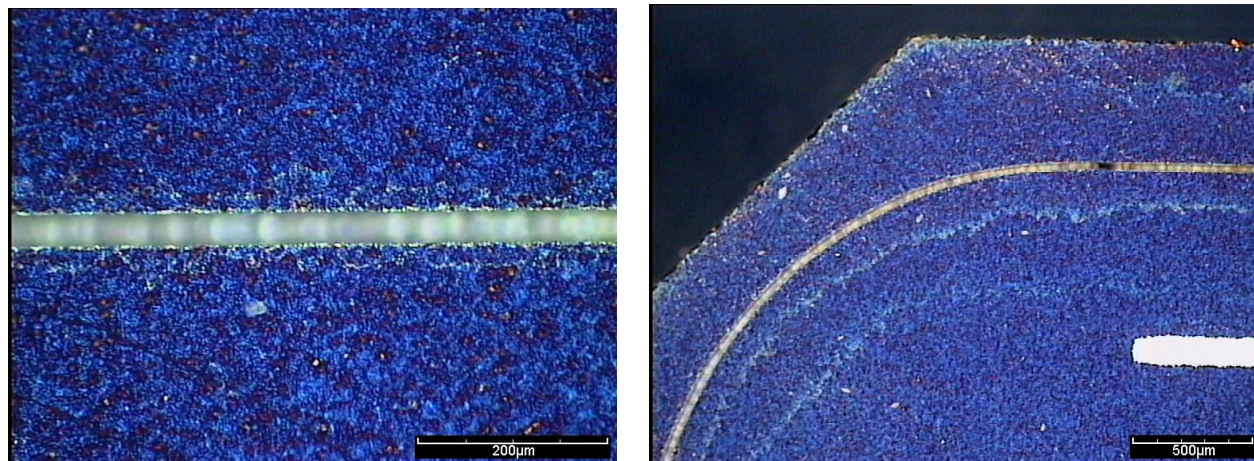


Fig. 8 Microscopic images of rounded groove cut at corner (l) and enlarged view of straight cut in silicon solar cell (r)

Cutting of Thick Silicon Wafer

This example shows the unique capabilities in cutting material that is not possible with conventional dry laser technology. The sample was high purity silicon wafer, 150mm diameter and 1200 μm thick. The cut was performed with a 532nm Q-switched laser and 50 μm nozzle at a speed of 200mm/s using 35 passes, giving an overall speed of 5.71mm/s. The image in Figure 9 shows the sidewall of the sample, and traces of the cutting passes are clearly visible. The following Figure 10 shows the perfect front and back edges of the silicon after cutting, with minimal chipping evident.

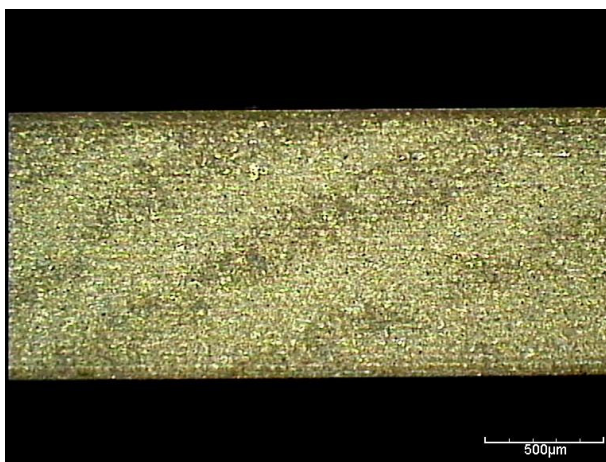


Fig. 9 Microscopic image of sidewall of 1200 μm thick pure silicon wafer

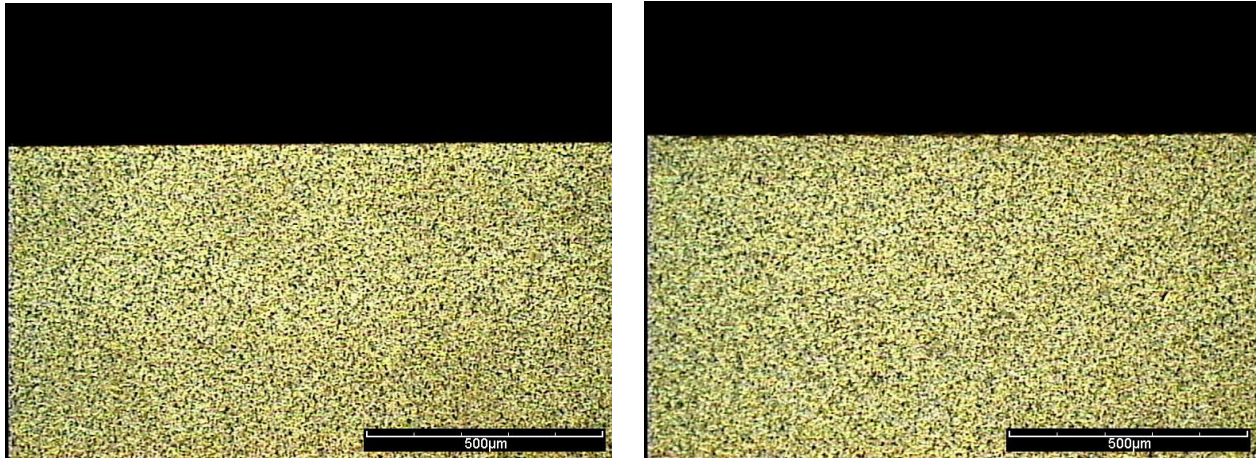


Fig. 10 Microscopic image of front (l) and back (r) edges of the 1200µm thick pure silicon wafer

Cutting of Polychrystalline Diamond/Tungsten 3.6mm Thick 58mm Diameter Disk

This example illustrates the LMJ capabilities when used for cutting super hard materials such as Polychrystalline Diamond (PCD) on a Tungsten (WC) backing. The cuts were made with a frequency doubled Nd:YAG laser, using an 80µm nozzle in a multi/pass mode. Cutting speed was 3.3 mm/min. Figure 11 shows the resulting sidewall after cutting of the material and the high quality results obtained.

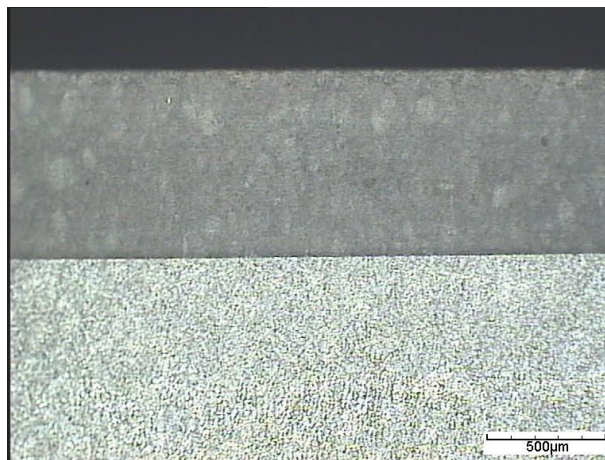


Fig. 11 Microscopic image of the sidewall cut of the PCD/WC material

Percussion drilling of blind holes in silicon wafers

In Figure 12 the consistency of the percussion drilling results on a 600µm thick bare silicon wafer using a third harmonic 355nm UV laser are shown.

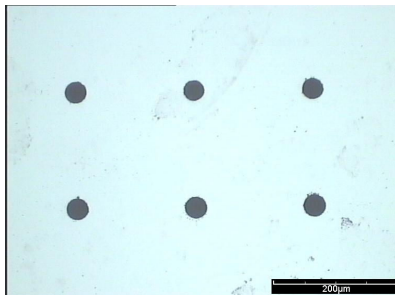


Fig. 12 A hole matrix, top view, 30 µm nozzle, 90 kHz, 9 W, 20 holes/s

The average measured hole diameter is 35µm, and hole circularity is about 0.9. With no post cleaning steps, the holes are clean and free of debris, burrs, cracks and thermal damage. The hole diameter at the bottom is about 15µm. The depth of the holes is approximately 50µm.

Very small holes were also generated on the metallic contact pads of a 700µm thick device wafer shown in Figure 14. A 1070µm fibre laser was selected for this experiment, producing 70µm deep and 30µm diameter holes.

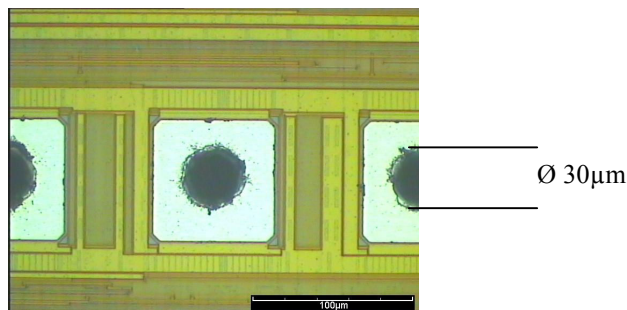


Fig. 13 Holes drilled in metallic contact pads, 25 µm nozzle, 26W, 50 kHz, 30 holes/s

References

- [1] Richerzhagen B. (2001), Chip singulation process with a water-jet guided laser, *Solid State Technology* 44(4), S25–S28.
- [2] Colladon D. (1842), “On the reflections of a ray of light inside a parabolic liquid stream”. *CR Hebd Séanc Acad Sci Paris* 15:800-802.
- [3] Snyder A.W. & Love J.D. (1983), *Optical Waveguide Theory*, Chapman and Hall, New York.
- [4] Snyder A.W. (1972), Coupled mode theory for optical fibers, *J. Opt. Soc. Am.* 62(11), 1267.
- [5] Sterling A.M. & Sleicher C. A. (1975), The instability of capillary jets, *J. Fluid Mech.* 68(3), 477–495.
- [6] Couty Ph., Vago N., Spiegel A., Ugurtas B.I. & Hoffmann P. (2003), Laser induced breakup of water-jet waveguide, *In press Exp. Fluids*.
- [7] Vennard J.K. & Street R.L. (1976), *Elementary Fluid Mechanics*, John Wiley & Sons, New York, 157-158; 557-563.
- [8] Yarin A.L. (1993), Hydrodynamic phenomena in liquid jets and films. In: *Free liquid jets and films: hydrodynamics and rheology*, ch. 1, pp 4-7, London: Longman and Wiley
- [9] Lin S.P. & Reitz R.D. (1998), Drop and spray formation from a liquid jet. *Annu Rev Fluid Mech* 30: 85-105
- [10] Taub H.H. (1976), Investigation of nonlinear waves on liquid jets. *The Phys Fluids* 19: 1124-1129
- [11] Xing J.H., Boguslawski A., Soucemarianadin P. & Attané P. (1996), Experimental investigation of capillary instability: results on jet stimulated by pressure modulations. *Exp Fluids* 20: 302-313
- [12] Goedde E.F. & Yuen M.C. (1970), Experiments on liquid jet instability. *J Fluid Mech* 40: 495-511
- [13] Lafrance P. (1975), Nonlinear breakup of a laminar liquid jet. *The Phys Fluids* 18: 428-432
- [14] Leroux S., Dumouchel C. & Ledoux M. (1996), The stability curve of Newtonian liquid jets. *Atom Sprays* 6: 623-647

Biographies

Dr. Tuan Anh Mai

Tuan Anh Mai received his Dipl.-Ing. (MSc) in mechanical engineering at the University of Ilmenau (Germany) and his Dr.-Ing. (PhD) in materials engineering at the University of Hannover (Germany). Dr. Mai has been working in the field of optics and laser materials processing, more specifically in developing and customizing laser micro-machining processes and systems since 1984. He worked at the Laser Zentrum Hannover and Singapore Institute of Manufacturing Technology as a research scientist and project manager. Before joining Synova as an R&D Manager, he worked in the Netherlands for a laser wafer dicing company as Process Development and Application Manager.

Dr. Nándor Vágó

Nándor Vágó received his MS degree in engineering physics from the Budapest University of Technology and Economics and started PhD school in 1999. With a Swiss federal scholarship he continued his PhD research at the Swiss Federal Institute of Technology in Lausanne in a joint research program with Synova SA from January 2000. His research interest is in microjet stability.

Dr. Bernold Richerzhagen

Bernold Richerzhagen received his M.Sc. in mechanical engineering from Aachen Polytechnic in Germany (RWTH) and his Ph.D. in micro-technology from the Swiss Federal Institute of Technology Lausanne. He became CEO of Synova SA in 1997. He is acknowledged as the inventor of water jet-guided laser technology.

Mr. Notker U. Kling

Notker Kling is the General Manager for Synova’s North America activities. He has extensive international experience in leading high-technology companies, where he has held numerous management and executive positions at companies such as Leybold, BPS, Unaxis and Singulus in Europe, Asia and North America. He holds a diploma in Electrical Engineering and Information Technology from the University Giessen-Friedberg.

Mr. Keith Stay

Keith Stay is the Technical Writer with Synova SA.